doi:10.1017/S1431927619008043
Microsc. Microanal. 25 (Suppl 2), 2019


# Influence of Water Vapor on NiAl Oxidation Using *in situ* STEM

Kinga A. Unocic[1*], Franklin S. Walden II[2] and Lawrence F. Allard[1]

[1.] Center for Nanophase Materials Sciences, Oak Ridge National Laboratory, Oak Ridge, TN, USA.
[2.] Protochips Inc., Morrisville, NC, USA.
[*] Corresponding author: unocicka@ornl.gov

From a materials degradation perspective, there is sustained interest in studying the influence of water vapor on the high-temperature oxidation of structural materials used in gas turbine engines since a major product of hydrocarbon fuel combustion is water vapor [1,2]. Previous research has shown that both Fe- and Ni-based alloys are prone to accelerated oxidation in the presence of water vapor [1-3]. For example, NiAl is a high-temperature structural material that forms a protective $Al_2O_3$ layer during high-temperature oxidation but this oxidation behavior is accelerated by water vapor [2,3]. Determination of the underlying oxidation mechanisms is most often elucidated through post-mortem electron microscopy and microanalysis-based characterization approaches. The aim of this study is to develop *in situ* closed gas-cell microscopy methods to investigate the influence of water vapor on high-temperature oxidation mechanisms and to quantify the oxidation kinetics *during* the reaction.

To perform the experiments we used a commercially available *in situ* S/TEM system (Protochips Atmosphere$^{TM}$), which was modified to allow for water vapor delivery and a residual gas analyzer (RGA) to track gas compositions [4]. To obtain a mixture of 10% of water vapor with $O_2$ at room temperature (RT) and without condensation along the supply and delivery lines, the total pressure was set to 170 Torr. This allowed us to mix 17 Torr (10%) of water vapor and 153 Torr (90%) of $O_2$ [4]. The mixing capability allowed us to obtain a final gas composition of 8%$H_2O$-92%$O_2$, which is typically used in high-temperature oxidation experiments. A nominal 50-50 NiAl system was used. The mass spectrum acquired during testing is shown in Fig. 1; an increased partial pressure $H_2O$ peak at 18 amu supports the presence of water vapor in the gas-cell (spectrum acquired without water vapor is also included). Figure 2 shows a series of bright-field (BF) STEM images of a particle of NiAl within the gas cell. Energy dispersive X-ray spectroscopy (EDS) was used to investigate the elemental distribution within the particle before and after oxidation – EDS maps shown in Fig. 3a correspond to the NiAl particle shown in Fig. 2a. A uniform distribution of Ni and Al was evident but the shape and thickness of the NiAl was irregular, which is not ideal for extracting kinetic parameters. A time-lapsed BF-STEM image series reveals the behavior of NiAl at 750°C in a flowing mixture of 8%$H_2O$-92%$O_2$ at 170 Torr (Fig. 2b). A uniform oxide layer formed on the NiAl surface that is evident after 581s (Fig. 3b). Additionally, accelerated oxidation initiated at the tip of the NiAl particle and at specific locations along edge of the NiAl (arrows in Fig. 2b, 60s frame). The higher rate of reactivity at the tip was due to a limited reservoir of Al due to the geometry of the particle. The higher oxidation rates at other locations along the edge of the NiAl were due either to localized compositional differences near the surface or to flaws related to the sample preparation. In the accelerated oxidation locations, oxidation progressed in a faceted fashion (Fig. 2b, 581s and 2321s frames). After 2321s, other local areas oxidized at faster rates due to the continued depletion of the Al reservoir. Figure 3b shows EDS elemental maps after oxidation that indicate shrinking of the NiAl, suggesting inward diffusion of $Ni^{2+}$ ions and outward diffusion of $Al^{3+}$ to the oxide/metal interface. Results demonstrate *in situ* S/TEM reaction of structural materials with water vapor at pressures higher than a few Torr [6].

References:
[1] BA Pint et al., Surface & Coatings Tech. **201** (2006), p. 3852.
[2] R Kartono and D Young, ECS Proceedings **16** (2004), p. 43.

[3] I Kvernes et al., Corros. Sci. **17** (1977), p. 237.
[4] KA Unocic et al., Micros. Microanal. **24** Suppl. 1 (2018), p.286.
[5] KA Unocic et al., Oxid. Metals **88** (2017), p. 495.
[6] Research sponsored by Oak Ridge National Laboratory's Laboratory Directed Research and Development Program, managed by UT-Battelle, LLC for the U.S. Department of Energy.

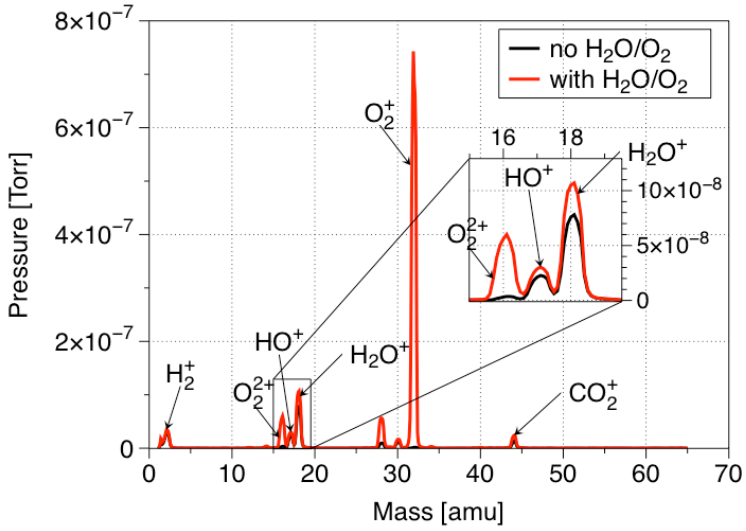


**Figure 1.** Mass spectra acquired *before* (black spectrum) and *during* (red spectrum) flowing $O_2$ with $H_2O$ (8%$H_2O$-92%$O_2$) through the gas cell. Mass spectra acquired by RGA system on the exit side of the TEM holder.

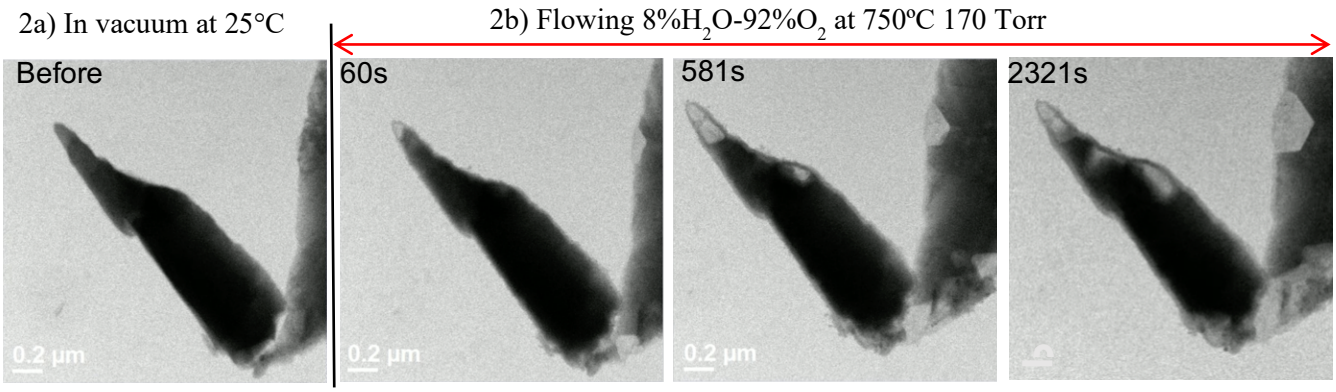


**Figure 2.** BF-STEM images of NiAl particle (a) at RT and (b) time-lapsed images showing same NiAl particle exposed at 750°C in flowing mixture of 8%$H_2O$-92%$O_2$ at 170 Torr.

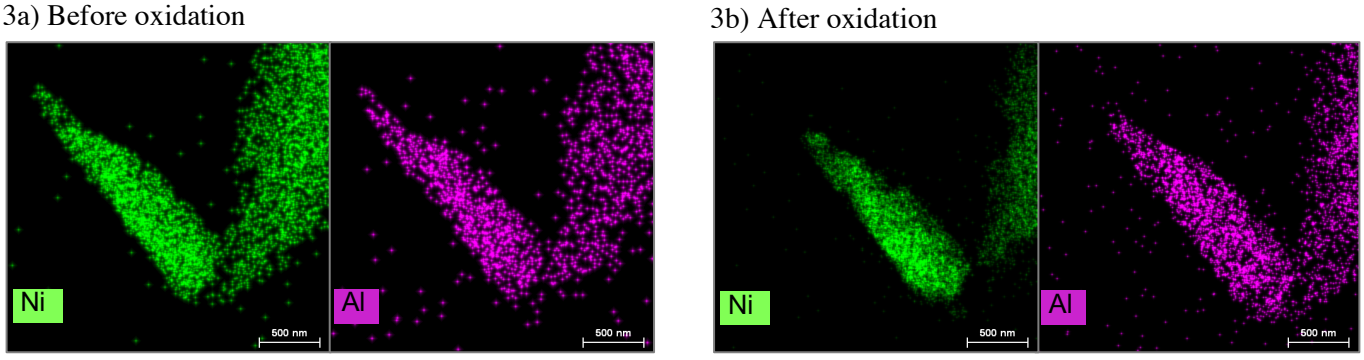


**Figure 3.** Ni and Al elemental maps for (a) fresh NiAl particle shown in Figure 1 at RT in vacuum and (b) after exposure at 750°C in flowing 8%$H_2O$-92%$O_2$ and 170 Torr.

https://doi.org/10.1017/S1431927619008043 Published online by Cambridge University Press